

# Make Domain Shift a Catastrophic Forgetting Alleviator in Class-Incremental Learning

Wei Chen<sup>1,2</sup>, Yi Zhou<sup>1,2</sup>\*

<sup>1</sup>School of Computer Science and Engineering, Southeast University, China

<sup>2</sup>Key Laboratory of New Generation Artificial Intelligence Technology and Its Interdisciplinary Applications, Ministry of Education, China  
weighchen@seu.edu.cn, yizhou.szc@gmail.com

## Abstract

In the realm of class-incremental learning (CIL), alleviating the catastrophic forgetting problem is a pivotal challenge. This paper discovers a counter-intuitive observation: by incorporating domain shift into CIL tasks, the forgetting rate is significantly reduced. Our comprehensive studies demonstrate that incorporating domain shift leads to a clearer separation in the feature distribution across tasks and helps reduce parameter interference during the learning process. Inspired by this observation, we propose a simple yet effective method named DisCo to deal with CIL tasks. DisCo introduces a lightweight prototype pool that utilizes contrastive learning to promote distinct feature distributions for the current task relative to previous ones, effectively mitigating interference across tasks. DisCo can be easily integrated into existing state-of-the-art class-incremental learning methods. Experimental results show that incorporating our method into various CIL methods achieves substantial performance improvements, validating the benefits of our approach in enhancing class-incremental learning by separating feature representation and reducing interference. These findings illustrate that DisCo can serve as a robust fashion for future research in class-incremental learning.

**Code** — <https://github.com/PixelChen24/DisCo>

## 1 Introduction

Deep neural networks excel in static environments but falter with the dynamic nature of real-world data. Designed to learn from static datasets, these models struggle to adapt to new data without complete retraining. This leads to performance degradation and catastrophic forgetting (McCloskey and Cohen 1989) in real-world applications with continuously updated data (Luo et al. 2024). Continual learning, also known as incremental or lifelong learning, addresses this by allowing models to learn incrementally, retaining knowledge over time, and adapting to evolving data.

Generally, continual learning can be mainly taxonomized as **Class-Incremental Learning (CIL)** and **Domain-Incremental Learning (DIL)**. CIL (Zhou et al. 2022; Kirkpatrick et al. 2017; Rusu et al. 2016; Wang et al. 2022c)

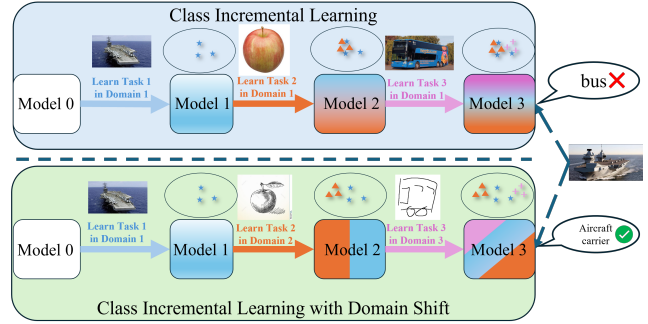


Figure 1: The key finding of our work: Incorporating domain shift in class incremental learning contributes to a clear separation of feature space and a better resistance to forgetting.

involves learning a sequence of tasks, with each task only introducing new classes that were not present in the previous tasks. The model should correctly classify new samples into all classes seen so far. Unlike CIL which focuses on expanding the model’s class knowledge, DIL (Tang et al. 2021; Tao et al. 2020; Volpi, Larlus, and Rogez 2021) requires the model to generalize effectively across varying data distributions (Lai et al. 2024; Liu and Zhou 2024) with the same label space and fight against forgetting at the same time. There is no doubt that combination of CIL and DIL can better simulate the real world where new knowledge and new data distribution are introduced gradually. Relatively a few studies have been conducted to provide solutions to this combination. Many works (Kundu et al. 2020; Simon et al. 2022; Xie, Yan, and He 2022) explore various problem settings of combining CIL with DIL, emphasizing adaptation and generalization across known and unknown domains. However, they did not really focus on the **effect of domain shift on CIL**. Thus, we are motivated by this question: “Does domain shift really hamper CIL methods?”

In this work, we first discover that domain shift helps reduce the interference and forgetting across tasks in CIL, as illustrated in Fig. 1. Specifically, we start with an empirical study where we simulate the combination of CIL and domain shift by splitting DomainNet (Peng et al. 2019) dataset, or manually add domain shift using a style transfer GAN to the original CIFAR-100 dataset (Krizhevsky

\*Corresponding author

and Hinton 2009) to construct DomainCIFAR-100. Qualitative results on DomainNet and DomainCIFAR-100 show that domain shift assists model in learning distinguishable representations across tasks. To further investigate the effects of domain shift, we design a quantitative metric to measure the interference across tasks, along with a metric to measure the knowledge learned by the model. We find that domain shift helps reduce the interference during parameter updating and improves the knowledge transfer, thus reducing forgetting rate. Then, we leverage this discovery to design a simple yet effective plug-and-play method named **DisCo** (Distinguishable feature for Continual Learning) to deal with CIL tasks. DisCo utilizes contrastive loss to impose task-level and class-level regularization on prototypes to foster distinguishable task representations. DisCo also includes a cross-task contrastive distillation loss to preserve prior knowledge effectively. DisCo can be easily integrated into existing state-of-the-art continual learning methods, especially rehearsal-based methods, to boost performance. We perform extensive experiments on popular CIL benchmarks and show that incorporating DisCo reduces forgetting significantly and improves their performance consistently.

**Our contributions are highlighted as follows:** **1)** We observe the counter-intuitive phenomenon that when introducing domain shift to the standard CIL setting, the overall forgetting is significantly reduced. To the best of our knowledge, we’re the first to discover this phenomenon. **2)** Through analyzing the parameter updated during sequential tasks, we find that the task interference is small due to the variance caused by the domain shift of input, which consequently leads to a relatively lower forgetting rate. **3)** Based on our observation, we introduce a simple yet effective plug-and-play method named DisCo, which can be easily integrated into existing class-incremental methods to hedge against forgetting.

## 2 Related Works

**Class-Incremental Learning.** In class-incremental learning, models are continuously updated with new class data, aiming to retain performance on previously learned classes without the original training data. Various strategies address forgetting (Wang et al. 2024), including rehearsal-based methods, which use a memory buffer to store exemplars (Rebuffi, Kolesnikov, and Lampert 2016; Caccia et al. 2020; Zhou et al. 2022) or generate images of old classes using generative networks (Van de Ven, Siegelmann, and Tolia 2020; Liu et al. 2020). Regularization-based approaches implement weight regularization on important parameters (Kirkpatrick et al. 2017; Lin, Chu, and Lai 2022) or knowledge distillation to preserve crucial outputs (Li and Hoiem 2017; Wang et al. 2022a). Architecture-based methods expand (Buzzega et al. 2020; Mallya and Lazebnik 2018; Rusu et al. 2016) or reallocate (Golkar, Kagan, and Cho 2019) the model’s structure to accommodate new tasks. Meanwhile, recently popular prompt-based methods (Smith et al. 2023; Wang et al. 2022b; Razdaibiedina et al. 2023), such as L2P (Wang et al. 2022c) guide pre-trained Transformers with task-specific prompts to balance shared and task-specific knowledge. Mixed strategies, like

DER (Buzzega et al. 2020), combine two or more strategies above to achieve a more robust continual learner.

**Contrastive Learning in Continual Learning.** Contrastive loss has been integrated into continual learning methods to combat catastrophic forgetting, with approaches like Co2L (Cha, Lee, and Shin 2021), which utilizes supervised contrastive loss for task learning paired with self-supervised loss for knowledge distillation between models. DualNet (Pham, Liu, and Hoi 2021) employs both supervised and self-supervised losses in training its fast and slow learners respectively, enhancing generalizable representations. These methods operate on the assumption that contrastive loss yields more stable representations for future tasks compared to cross-entropy loss (Cha, Lee, and Shin 2021). Our research, however, focuses on the utility of contrastive loss in learning discriminative features across tasks.

**Domain Shift in Class-Incremental Learning.** The intersection of class-incremental and domain-incremental learning has been sparingly explored. Kundu’s work (Kundu et al. 2020) blends class-incremental learning with source-target domain adaptation, specifically designed for open-set environments. Meanwhile, Xie (Xie, Yan, and He 2022) has crafted a comprehensive framework that concurrently addresses the challenges posed by both class and domain continual learning. Building on this, Simon (Simon et al. 2022) introduces a method that not only addresses cross-domain continual learning but also ensures robust generalization to new, unseen domains. Despite these innovative approaches, the literature still lacks a detailed exploration of how domain shift specifically affects class-incremental learning.

## 3 Empirical Study

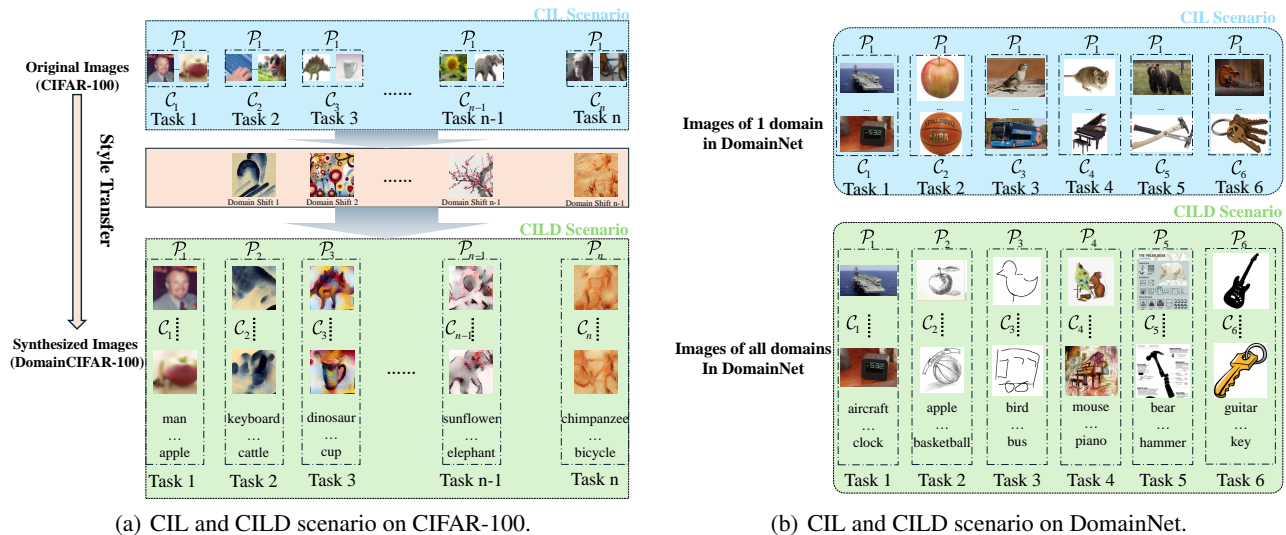
### 3.1 Problem Setup

Here we first introduce the formal definition of standard **Class-Incremental Learning (CIL)**. Let  $\mathcal{D} = \{D_1, D_2, \dots, D_T\}$  represent a sequence of datasets corresponding to tasks  $1, 2, \dots, T$ . Each dataset  $D_t = \{(x_i^t, y_i^t)\}_{i=1}^{N_t}$  consists of  $N_t$  samples, where  $x_i^t$  is the  $i$ -th input and  $y_i^t$  is the corresponding label from the label set  $\mathcal{C}_t$ . For each task  $T_t$ , the label space  $\mathcal{C}_t$  introduces new classes, and  $\mathcal{C}_t \cap \mathcal{C}_{t'} = \emptyset$  for  $t \neq t'$ . Thus, the cumulative label space up to task  $t$  is  $\mathcal{C}^t = \bigcup_{k=1}^t \mathcal{C}_k$ . Model at task  $t$  only has access to  $D_t$ , and the goal at task  $t$  is to train a model  $f_\theta^t$  parameterized by  $\theta_t$  which can classify inputs  $x$  into the correct class among all classes  $\mathcal{C}^t$  seen so far. Formally, after training on  $D_T$ , the model  $f_\theta^T$  should minimize the loss:

$$\mathcal{L}(\theta) = \sum_{t=1}^T \sum_{(x_i^t, y_i^t) \in D_t} L(f_\theta^T(x_i^t), y_i^t), \quad (1)$$

where  $L$  is a loss function appropriate for classification.

Most previous CIL works conduct experiments under the setting that all tasks share the same distribution, i.e.  $\mathcal{P}_t = \mathcal{P}_{t'}$ , for  $t \neq t'$  and overlook the effect of domain shift on CIL. We are interested in this question: What if the  $\mathcal{P}$  is different from each other? i.e.,  $\mathcal{P}_t \neq \mathcal{P}_{t'}$ ,  $\forall t \neq t'$ .



(a) CIL and CILD scenario on CIFAR-100.

(b) CIL and CILD scenario on DomainNet.

Figure 2: Illustration of two scenarios construction on two datasets respectively. In Fig. 2(a), we use AvatarNet (Sheng et al. 2018) to synthesize images of new domains on CIFAR-100. We use the original images as training/testing set for CIL scenario and synthesized images (termed DomainCIFAR-100) as training/testing set for CILD scenario. In Fig. 2(b), we split DomainNet (Peng et al. 2019) to construct CIL and CILD scenario. Images of one domain make up the training/testing set for CIL scenario, and images of all domains make up the training/testing set for CILD scenario. In each dataset, the label space  $C_t$  of each task  $t$  in CILD is consistent with that of CIL.

### 3.2 Observation of Domain Shift on CIL

To investigate the effect of domain shift in class-incremental learning methods, we first illustrate some analytical experiments on CIFAR-100 (Krizhevsky and Hinton 2009) and DomainNet (Peng et al. 2019) under two scenarios.

**Empirical Study Setup.** We design two comparative scenarios: the classic CIL scenario and an extended version incorporating domain shift, which we term **Class Incremental Learning with Domain shift (CILD)**.

- **CIL:** Tasks are introduced sequentially without any alteration to the domain, following standard CIL setting.
- **CILD:** Based on CIL, each task  $t$  is modified by introducing a unique variation in the domain while sharing the same label space  $C_t$  with CIL. As shown in Fig. 2, we construct CILD in two ways: 1) Synthesizing. We use a pre-trained style transfer model to transfer the original image of CIFAR-100 to multiple domains and use the synthesized dataset DomainCIFAR-100 for training and inference. 2) Splitting. We split an existing dataset with domain variation (Peng et al. 2019) to form a task sequence. Appendix B.1 shows more details about the CILD scenario setup.

**Evaluation Protocols.** In general, we consider the performance of continual methods from two aspects (Wang et al. 2024): the overall Average Accuracy  $AA$  of the tasks learned so far, and the forgetting measure  $FM$  of old tasks.  $AA$  evaluates the ability to learn new classes while  $FM$  reflects the performance drop of old classes. A lower  $FM$  means the model is more robust to fight against forgetting and a higher  $AA$  means the model performs well both in

learning new knowledge and preserving old knowledge. The detailed mathematical definition of these two metrics can be found in the Appendix A.1.

**Observation.** For the baseline CIL methods, we select six representative methods: iCaRL (Rebuffi, Kolesnikov, and Lampert 2016), BiC (Wu et al. 2019), MEMO (Zhou et al. 2022), LwF (Li and Hoiem 2017), DER (Buzzega et al. 2020), and L2P (Wang et al. 2022c), covering four different method categories as discussed in sec 2. Details of these methods' implementation can be found in Appendix C.2.

As shown in Tab. 1, most CIL methods under CILD demonstrate significantly lower forgetting compared to CIL. This phenomenon is not restricted to a single model or method, and we observe consistent results across various methodologies, regardless of their backbone types or whether pretrained. Note that  $AA$  of CILD is generally lower than that of CIL because we use the synthesized images or images belonging to weird domains which may be hard to classify for task  $t \geq 2$  in CILD. This leads to a lower initial accuracy of these tasks and a lower  $AA$  consequently. If we take a close look at just the first task performance during the whole process, we can observe that the model suffers from much less forgetting under CILD. Details of these observations above can be found in Appendix B.3.

Despite the fantastic low  $FM$  of most methods under the CILD scenario, prompt-based method like L2P seems to be the exception, which is more prone to forgetting. This can be attributed to the fact that the backbone remains frozen during the training of prompt-based methods and the key-prompt pairs are the only tunable parameters. These parameters have much less scalability compared to the pre-trained

Method	Scenario	CIFAR-100				DomainNet			
		$AA \uparrow$	$FM \downarrow$	$PIV \downarrow$	$PFTS \uparrow$	$AA \uparrow$	$FM \downarrow$	$PIV \downarrow$	$PFTS \uparrow$
iCaRL	CIL	58.94	59.42	73.50	23.87	57.41	41.27	74.00	27.85
iCaRL	CILD	<b>61.19</b>	<b>25.98(-33.44)</b>	<b>56.00</b>	<b>29.54</b>	<b>63.32</b>	<b>22.88(-18.39)</b>	<b>57.00</b>	<b>36.11</b>
BiC	CIL	70.53	42.80	69.00	56.21	<b>62.54</b>	36.20	76.50	54.39
BiC	CILD	<b>72.16</b>	<b>16.04(-26.76)</b>	<b>53.00</b>	<b>77.25</b>	61.82	<b>13.12(-23.08)</b>	<b>64.00</b>	<b>56.03</b>
MEMO	CIL	<b>89.87</b>	16.91	72.50	68.24	<b>91.40</b>	10.67	73.00	68.84
MEMO	CILD	86.38	<b>7.56(-9.35)</b>	<b>62.50</b>	<b>95.30</b>	86.67	<b>8.31(-2.36)</b>	<b>72.00</b>	<b>95.30</b>
LwF	CIL	<b>50.49</b>	49.35	32.00	35.80	<b>48.62</b>	46.58	36.50	39.65
LwF	CILD	48.02	<b>23.48(-25.87)</b>	<b>28.50</b>	<b>46.59</b>	45.00	<b>27.30(-19.28)</b>	<b>26.00</b>	<b>43.08</b>
DER	CIL	62.51	40.26	1.00	5.11	67.55	34.21	1.00	6.19
DER	CILD	<b>72.02</b>	<b>0.50(-39.76)</b>	1.00	<b>6.33</b>	<b>69.73</b>	<b>9.56(-24.65)</b>	1.00	<b>10.57</b>
L2P	CIL	<b>91.36</b>	<b>4.42</b>	100.00	30.16	<b>91.35</b>	<b>3.81</b>	100.00	28.55
L2P	CILD	61.37	13.46(+9.04)	100.00	<b>59.75</b>	83.51	5.04(+1.23)	100.00	<b>52.70</b>

Table 1: Comparative results on average accuracy ( $AA$ ), forgetting ( $FM$ ), interference ( $PIV$ ) and knowledge transfer ( $PFTS$ ) of CIL methods with(in gray rows) and without(in white rows) domain shift on CIFAR-100 and DomainNet.  $PIV$  and  $PFTS$  will be introduced in section 3.3.

encoder. When faced with examples within the data distribution where the encoder is trained, prompts can adapt to them easily by introducing minor modifications with minor forgetting. But when the input sample style is significantly different from previous ones, these prompts tend to overfit these outlier samples and fail to preserve old knowledge.

Moreover, we use t-SNE (Van der Maaten and Hinton 2008) to visualize the feature representations of each task on CIFAR-100 in Fig. 3. In CIL, there is notable overlap among features of different tasks, indicating a struggle to maintain distinct task-specific features and leading to forgetting. In contrast, in CILD, features from different tasks are separated into well-defined clusters, demonstrating effective preservation of task uniqueness and reduced interference. This suggests that domain shifts help protect the knowledge of previous classes and reduce interference when learning new ones.

### 3.3 Quantitative Analysis

Inspired by the surprisingly low forgetting rate of CILD, one hypothesis is that just certain parts of the parameters are updated conditioned on the distinguishable input representations, thus reducing the interference between tasks. To quantify the interference among parameters that are heavily updated across different tasks, we design a metric named  $PIV$  (Parameter Interference Value) to capture how changes in one set of parameters affect the others across the sequence of tasks, and a metric named  $PFTS$  (Parameter Forward Transfer Score) to capture how much knowledge is relatively learned by model. For clarity, the mathematical definition of these two metrics is presented in Appendix A.2.

The last two columns in Tab. 1 demonstrate the  $PIV$  and  $PFTS$  of various continual methods under CIL and CILD. It is shown that 1) Methods under CILD demonstrate lower  $PIV$  compared to CIL, suggesting that domain shift helps reduce the interference across tasks. 2) Methods under CILD usually demonstrate higher  $PFTS$ , indicating that domain shift may be beneficial for the model to learn var-

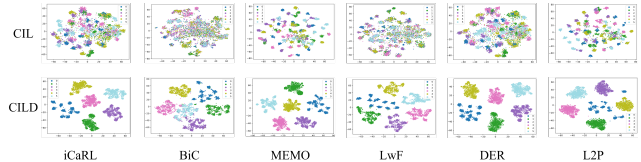


Figure 3: t-SNE visualization of features on CIFAR-100. The top row denotes features extracted by different continual methods under CIL scenario and the bottom row denotes features under CILD scenario. Data points from the same task are marked using the same color.

ious distinguishable representations in an ordered way. For architecture-based method DER,  $PIV$  under two settings are relatively lower because DER introduces new layers responsible for learning each task respectively. For prompt-based method L2P,  $PIV$  is 100% because a limited number of prompts are the only parameters that can be updated during training. At the same time, the  $PFTS$  is much higher than that under CIL, demonstrating the strong learning ability of the shared prompts. This leads to high interference across tasks in L2P and makes it perform worse under CILD.

## 4 Method

In section 3.2, we observed that domain shifts across tasks could significantly enhance the method’s resistance to forgetting in class-incremental learning. Integrating these domain shifts into existing CIL methods to boost performance is a natural idea. However, this raises a challenge: the model cannot determine which domain shift to apply to an input during inference. This resembles the paradigm of task-incremental learning (Wang et al. 2024), where the task ID (indicating the domain shift in our case) is needed at inference, which contradicts the CIL setting.

Instead, inspired by our observation, we propose to pro-



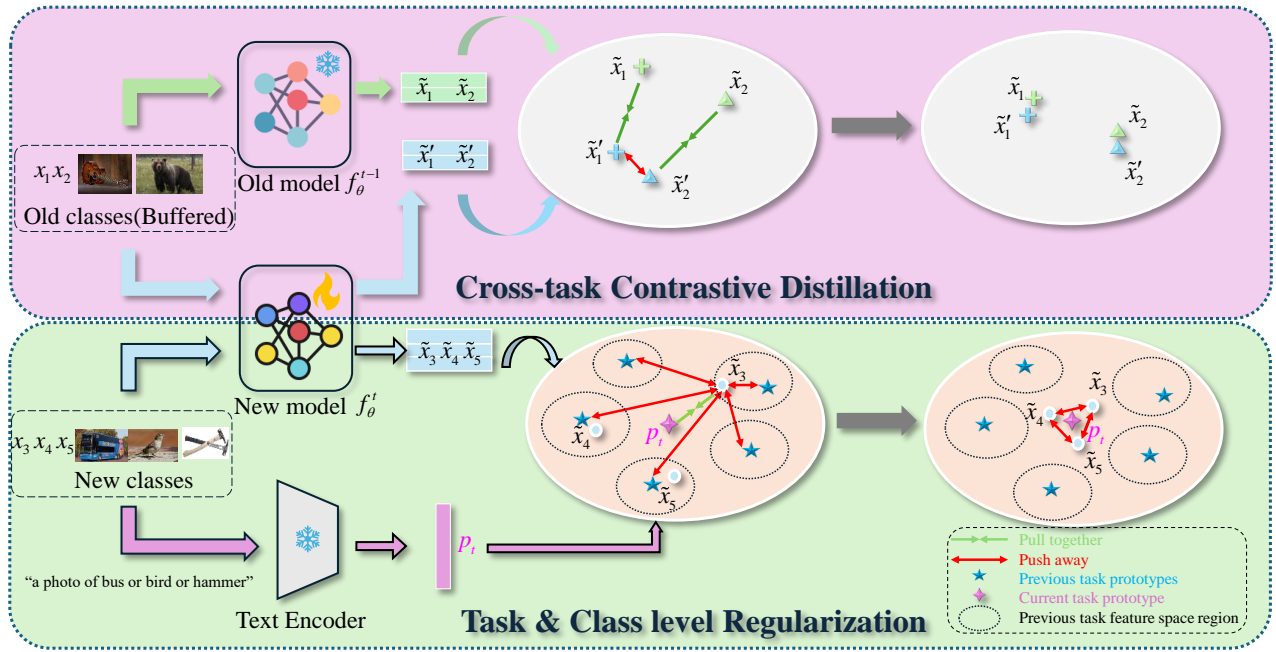


Figure 4: The overview framework of DisCo. DisCo includes Task&Class -level Regularization and Cross-task Contrastive Distillation. In Task&Class -level Regularization, samples in the current task are pulled toward the current task prototype while pushed away from previous task prototypes, leading to a discriminative feature distribution away from other tasks. Cross-task Contrastive Distillation helps align current model with previous one and preserve the features of old classes.

mote the differentiation of task-specific features and aim to simulate the beneficial effects of domain shift within the feature space rather than the input. Consequently, we introduce **DisCo (Distinguishable feature for Continual Learning)**, a simple yet effective rehearsal-based method employing contrastive learning to learn distinguishable representations for continual tasks. DisCo is built upon existing rehearsal-based baseline continual methods and can be easily incorporated into them. The core idea of DisCo is to enforce a margin between the feature distributions of the current categories and prototypes of previous categories, thereby preventing the interference of old knowledge. As shown in Fig. 4, DisCo comprises mainly two parts: task-level and class-level regularization and cross-task contrastive distillation.

**Prototype construction:** In our work, we try two types of prototype: text prototype and image feature prototype. For a class-incremental task at stage  $t$ , given a mini-batch with index  $i$  of  $N$  training samples  $D_t^i = \{(x_j, y_j)\}_{j=1}^N$ , where  $x_j \in \mathbb{R}^{3 \times H \times W}$  and  $y_j \in \mathbb{R}$  denote the image and numerical class label of the  $j$ -th sample respectively. We feed  $\{x_j\}_{j=1}^N$  into feature extractor  $\mathbf{F}_\theta^t$  to get their features  $\{\hat{x}_j\}_{j=1}^N \in \mathbb{R}^{N \times D}$ , followed by a projector  $\psi_t$  to project into a lower dimension space  $\{\tilde{x}_j\}_{j=1}^N \in \mathbb{R}^{N \times d}$ . The batch-wise image feature prototype  $p_i$  is then calculated as  $\frac{1}{N} \sum_{j=1}^N \tilde{x}_j$ .

For batch-wise text prototype, we collect all class names of this batch and feed the below text prompt to CLIP (Radford et al. 2021) text encoder to extract embedding  $p_i$ :

“a photo of {class 0} or {class 1} or ... or {class n}”

To let the batch-wise  $p_i$  approximate prototype  $P_i$  of the whole task, we calculate the momentum accumulation of  $p_i$ :

$$p_i = \frac{i-1}{i} p_{i-1} + \frac{1}{i} p_i \quad (2)$$

After all  $N_t$  mini-batches of task  $t$ ,  $p_{N_t}$  is stored in the prototype pool  $\mathbf{P}$  as the prototype  $P_t$  of task  $t$ .

#### 4.1 Task-level and Class-level Regularization

In task-level regularization, we aim to keep features of the current task away from the prototypes of previous tasks.

We treat each sample  $x_j$  in the  $i$ -th mini-batch as the anchor and treat the prototype  $p_i$  of this batch as the only positive sample  $x_{p_i}$ . Prototypes of all previous tasks  $P_k, \forall k < t$  are negative samples. As a result,  $N \times (t-1)$  pairs of triplets can be constructed in this mini-batch, and then task-level contrastive loss  $\mathcal{L}_{tcon}$  is:

$$\mathcal{L}_{tcon} = \frac{1}{N \times (t-1)} \sum_{j=1}^N \sum_{k=1}^{t-1} \text{Triplet}(x_j, p_i, P_k) \quad (3)$$

$$\text{Triplet}(a, p, n) = \log(1 + \exp(1 - S(a, p) + S(a, n))) \quad (4)$$

where  $S(x, y)$  is the cosine similarity function.  $\mathcal{L}_{tcon}$  ensures the feature space margin between the current task and previous ones, preventing task interference.

In class-level regularization, the goal is to learn discriminative features for each class in the current task. For each sample  $x_j$ , we randomly select a sample having the same label with  $x_j$  in this batch as the positive sample  $x_p$ , and select

a random negative sample  $x_n$  having a different label. Then the class-level contrastive loss  $\mathcal{L}_{cccon}$  is:

$$\mathcal{L}_{cccon} = \frac{1}{N} \sum_{j=1}^N \text{Triplet}(x_j, x_p, x_n) \quad (5)$$

## 4.2 Cross-task Contrastive Distillation

Despite the satisfactory performance achieved through the combined use of the aforementioned regularization and the rehearsal mechanism in the baseline method, the incorporation of an explicit mechanism to preserve acquired knowledge could yield further benefits. Here we leverage a Cross-task Contrastive Distillation loss(CCD) to help align the current student model with the old teacher model. At task  $t$ , we copy the trained model of task  $t - 1$  as the teacher model  $f_{\theta}^{t-1}$  which remains frozen during task  $t$ , and the current model  $f_{\theta}^t$  serves as the student model. The contrastive distillation aims to align the feature representation of the student model and teacher model for old classes, preventing the degradation of old classes’ features. Specifically, for a sample  $x_j$  in the rehearsal sample set  $\mathcal{R} = \{(x_j, y_j) | y_j \notin \mathcal{C}_t\}$ , we use the teacher model  $f_{\theta}^{t-1}$  and student model  $f_{\theta}^t$  to extract their features, denoted as  $\tilde{x}_j$  and  $\tilde{x}_j'$ . The contrastive distillation loss is written as:

$$\mathcal{L}_{ccd} = \sum_{(x_j, y_j) \in \mathcal{R}} \sum_{k \in \mathcal{R}, y_k \neq y_j} \text{Triplet}(\tilde{x}_j', \tilde{x}_j, \tilde{x}_k') \quad (6)$$

$\mathcal{L}_{ccd}$  places restrictions on current student model to distill knowledge of the same old class from teacher model and simultaneously keep away from other different old classes.

## 4.3 Generalize to Various Types of CIL Methods

DisCo not only works well on rehearsal-based continual methods but also can generalize to other categories, such as regularization-based and prompt-based methods. For regularization-based methods, DisCo can be directly incorporated discarding CCD with minor performance degradation. For prompt-based methods such as L2P (Wang et al. 2022c), we just need to impose regularization on selected prompt keys like Eq. 3 instead of image features. More details about incorporating DisCo into prompt-based methods can be found in Appendix C.3.

As a result, the total loss  $\mathcal{L}$  of DisCo is:

$$\mathcal{L}_{baseline} + \lambda_{tcon} \mathcal{L}_{tcon} + \lambda_{cccon} \mathcal{L}_{cccon} + \lambda_{ccd} \mathcal{L}_{ccd} \quad (7)$$

where  $\mathcal{L}_{baseline}$  refers to the vanilla loss of the baseline continual method,  $\lambda_{tcon}$ ,  $\lambda_{cccon}$  and  $\lambda_{ccd}$  are hyperparameter to balance these losses. In our experiments,  $\lambda_{tcon}$  and  $\lambda_{cccon}$  are set to 0.5 and  $\lambda_{ccd} = 1$ . Evaluations of other possible values are reported in Appendix C.5.

# 5 Experiments

## 5.1 Experiment Setup

**Datasets and Implementation:** We perform experiments on CIFAR100, Fashion-MNIST, and Tiny-ImageNet. Details of these datasets and continual task split are in Appendix C.1.

Method	CIFAR100		FashionMNIST		TinyImageNet	
	AA $\uparrow$	FM $\downarrow$	AA $\uparrow$	FM $\downarrow$	AA $\uparrow$	FM $\downarrow$
iCaRL	64.24	51.34	69.41	47.44	8.57	81.40
iCaRL + Disco-I	<b>70.11</b>	<b>33.96</b>	<b>72.57</b>	34.45	10.87	<b>70.19</b>
iCaRL + Disco-T	63.35	35.26	70.69	<b>33.65</b>	<b>11.88</b>	70.46
BiC	67.04	46.51	73.63	38.77	<b>8.42</b>	78.42
BiC + Disco-I	<b>69.89</b>	28.54	73.24	<b>34.22</b>	8.16	68.05
BiC + Disco-T	67.68	<b>23.08</b>	<b>74.18</b>	35.00	8.33	<b>67.94</b>
Co2L $^\dagger$	71.25	32.17	68.54	34.66	14.02	74.55
LwF	51.30	55.98	53.15	51.27	5.06	85.50
LwF + Disco-I	56.42	36.52	<b>57.14</b>	<b>37.69</b>	<b>7.87</b>	79.58
LwF + Disco-T	<b>56.87</b>	<b>33.89</b>	52.87	44.11	6.22	<b>77.15</b>
DER	63.91	40.18	68.21	37.85	11.58	77.99
DER + Disco-I	64.87	36.41	<b>72.41</b>	<b>29.86</b>	12.08	<b>72.11</b>
DER + Disco-T	<b>69.51</b>	<b>33.74</b>	70.59	31.43	<b>12.86</b>	73.02
L2P	82.65	7.62	85.21	6.74	29.54	44.30
L2P + Disco-I	82.78	7.98	<b>86.15</b>	7.88	28.43	43.32
L2P + Disco-T	<b>83.12</b>	<b>6.80</b>	84.99	<b>6.07</b>	<b>31.88</b>	<b>40.00</b>

Table 2: Main result of incorporating DisCo into existing continual methods. We group the compared methods by their category(rehearsal-based, regularization-based, architecture-based, or prompt-based). Co2L $^\dagger$  is a compared rehearsal-based method leveraging contrastive loss. Disco-I means image features as prototypes and Disco-T means text features as prototypes, as described in section 4. Each result is averaged over 3 runs.

Our code is implemented in PyTorch and based on LAMDA-PILOT(Sun et al. 2023), which is an open-source framework for easily designing continual methods. We select iCaRL(Rebuffi, Kolesnikov, and Lampert 2016), BiC (Wu et al. 2019), LwF (Li and Hoiem 2017), DER(Buzzega et al. 2020), and L2P(Wang et al. 2022c) as baseline methods and integrate DisCo into them. We also compare our methods with the Co2L (Cha, Lee, and Shin 2021), which is a rehearsal-based method leveraging contrastive loss to learn stable representations. Appendix C.2 shows more details about these methods’ implementations. For both ResNet (He et al. 2016) and ViT (Dosovitskiy et al. 2020) -based models, we train all tasks for 100 epochs, 60-th and 80-th epochs being milestones. For models built on ResNet, we set weight decay  $w = 5e - 4$  and learning rate  $lr = 0.1$  with  $\times 0.1$  at milestones. For ViT-based models,  $w = 2e - 4$ ,  $lr = 1e - 3$  with  $\times 0.1$  at milestones.

## 5.2 Evaluation on Three Benchmarks

Tab. 2 shows the result of incorporating DisCo into existing continual methods. It can be observed that DisCo helps most methods alleviate forgetting (FM) and improves average accuracy (AA). Especially, DisCo can boost the performance of rehearsal-based methods significantly: increase AA by 5.87% and reduce FM by 17.38% for iCaRL on CIFAR-100, increase AA by 3.31% and reduce FM by 10.94% on Tiny-ImageNet. Moreover, plugging DisCo achieves comparable or even better performance compared to the contrastive-based related work Co2L (Cha, Lee, and

Method	DisCo			DisCo w/o Ccon			DisCo w/o Tcon			DisCo w/o CCD		
	AA $\uparrow$	FM $\downarrow$	IA $\uparrow$	AA $\uparrow$	FM $\downarrow$	IA $\uparrow$	AA $\uparrow$	FM $\downarrow$	IA $\uparrow$	AA $\uparrow$	FM $\downarrow$	IA $\uparrow$
iCaRL + DisCo-I	<b>70.11</b>	33.96	80.16	67.21	<b>32.15</b>	75.22	66.00	47.41	82.54	69.35	35.47	80.34
BiC + DisCo-I	<b>69.89</b>	28.54	75.21	63.32	<b>28.16</b>	72.52	65.15	44.25	74.67	67.33	26.68	76.10
LwF + DisCo-I	<b>56.42</b>	36.52	81.67	51.34	<b>35.99</b>	76.02	52.88	52.63	81.24	-	-	-
DER + DisCo-I	<b>64.87</b>	36.41	78.56	60.35	37.68	74.48	61.23	42.16	79.51	62.76	<b>35.16</b>	78.68
L2P + DisCo-T	83.12	<b>6.80</b>	85.43	81.16	6.75	84.36	<b>83.16</b>	7.87	86.49	-	-	-

Table 3: Ablation study on DisCo components on CIFAR-100. *IA* refers to the average Initial Accuracy of each task as in Appendix A.1. Tcon refers to task-level regularization, Ccon refers to class-level regularization and CCD refers to cross-task distillation. For each method row, we highlight the highest *AA* and lowest *FM*. For non-rehearsal-based methods, there is no ablation on CCD, which is marked as “-”.

Shin 2021). For regularization-based methods, DisCo works as well leveraging our task&class -level and their intrinsic regularization module, reducing *FM* by 22.09% for LwF on CIFAR-100 and 8.35% on Tiny-ImageNet.

Compared to image features as prototypes (DisCo-I), using task text features as prototypes (DisCo-T) performs better on prompt-based methods. There are several possible reasons: 1) L2P employs a prompt pool that serves as a bridge between the task’s data and the model, guiding the model’s focus toward the most relevant features for each task. Text features encapsulate high-level semantic information, and can effectively steer the model’s attention to conceptual similarities and distinctions between classes or tasks. 2) Prompt-based methods are inherently more flexible in handling text features since they often originate from NLP backgrounds. Thus, they can more effectively utilize text prototypes to guide the learning process across different tasks.

The improvement of average accuracy is smaller than that of the forgetting rate, partly because task-level regularization imposes stricter restrictions on the feature distributions, making it a little more difficult to classify new classes, i.e. low initial accuracy of each task. Ablation study of these regularization modules is shown in section 5.3. More additional results such as t-sne visualization and other findings are presented in Appendix C.4.

### 5.3 Ablation Study

**Ablation study on components of DisCo** We conduct an ablation study of task&class -level regularization and CCD on CIFAR-100 as shown in Tab. 3. Task level regularization (Tcon) plays the most important role in helping the model distinguish different tasks, greatly reducing the interference and forgetting rate *FM*. However, only using Tcon makes it difficult for the model to learn new knowledge, leading to a lower *IA* and a lower *AA* consequently. Class level regularization (Ccon) helps the model learn discriminative features for different classes in the same task, thus making it easier to learn new tasks i.e., higher *IA*, contributing to a higher *AA* together with Tcon. Moreover, we find that CCD also greatly helps maintain old class features and prototype distributions, leading to lower *FM* and higher *AA*.

**Ablation study on task length** We conduct experiments on different increment strategies on CIFAR-100. We separate these 100 classes into several groups as most works

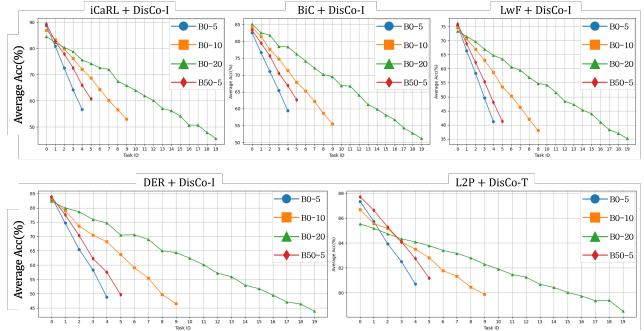


Figure 5: Ablation study on incremental task length.  $B\{X\}-\{Y\}$  means there are  $X$  classes in task 0 and the rest are evenly distributed in  $Y$  tasks. The y-axis means the  $AA_k$  at task  $k$ .

do(Rebuffi, Kolesnikov, and Lampert 2016; Wang et al. 2022c). Fig. 5 demonstrates that the forgetting trend is relatively milder as task length grows. This means DisCo can achieve good performance under different task length situations. Moreover, the forgetting trend of B50-5 is smaller than that of others, because DisCo relies on prototypes to guide the distribution of new tasks, the greater the sample number of each task is, the better performance DisCo achieves.

## 6 Conclusion

This paper demonstrates a counter-intuitive phenomenon: incorporating domain shift into class-incremental tasks significantly reduces catastrophic forgetting. Inspired by this, we propose DisCo, a contrastive learning-based simple yet effective plug-and-play method that effectively promotes distinct feature distributions for each task, mitigating interference and enhancing performance. Experimental results on various datasets show that DisCo can be easily integrated into other continual methods to boost performance.

## Acknowledgements

This work is supported in part by the National Natural Science Foundation of China under Grant 62476054, and in part by the Fundamental Research Funds for the Central Universities of China. This research work is supported by the Big Data Computing Center of Southeast University.

## References

- Buzzega, P.; Boschini, M.; Porrello, A.; Abati, D.; and Calderara, S. 2020. Dark experience for general continual learning: a strong, simple baseline. *Advances in neural information processing systems*, 33: 15920–15930.
- Caccia, L.; Belilovsky, E.; Caccia, M.; and Pineau, J. 2020. Online learned continual compression with adaptive quantization modules. In *International conference on machine learning*, 1240–1250. PMLR.
- Cha, H.; Lee, J.; and Shin, J. 2021. Co2l: Contrastive continual learning. In *Proceedings of the IEEE/CVF International conference on computer vision*, 9516–9525.
- Deng, J.; Dong, W.; Socher, R.; Li, L.-J.; Li, K.; and Fei-Fei, L. 2009. Imagenet: A large-scale hierarchical image database. In *2009 IEEE conference on computer vision and pattern recognition*, 248–255. Ieee.
- Dosovitskiy, A.; Beyer, L.; Kolesnikov, A.; Weissenborn, D.; Zhai, X.; Unterthiner, T.; Dehghani, M.; Minderer, M.; Heigold, G.; Gelly, S.; et al. 2020. An image is worth 16x16 words: Transformers for image recognition at scale. *arXiv preprint arXiv:2010.11929*.
- Golkar, S.; Kagan, M.; and Cho, K. 2019. Continual learning via neural pruning. *arXiv preprint arXiv:1903.04476*.
- He, K.; Zhang, X.; Ren, S.; and Sun, J. 2016. Deep residual learning for image recognition. In *Proceedings of the IEEE conference on computer vision and pattern recognition*, 770–778.
- Jaccard, P. 1901. Étude comparative de la distribution florale dans une portion des Alpes et des Jura. *Bull Soc Vaudoise Sci Nat*, 37: 547–579.
- Kirkpatrick, J.; Pascanu, R.; Rabinowitz, N.; Veness, J.; Desjardins, G.; Rusu, A. A.; Milan, K.; Quan, J.; Ramalho, T.; Grabska-Barwinska, A.; et al. 2017. Overcoming catastrophic forgetting in neural networks. *Proceedings of the national academy of sciences*, 114(13): 3521–3526.
- Krizhevsky, A.; and Hinton, G. 2009. Learning multiple layers of features from tiny images. *Handbook of Systemic Autoimmune Diseases*, 1(4).
- Kundu, J. N.; Venkatesh, R. M.; Venkat, N.; Revanur, A.; and Babu, R. V. 2020. Class-incremental domain adaptation. In *Computer Vision—ECCV 2020: 16th European Conference, Glasgow, UK, August 23–28, 2020, Proceedings, Part XIII 16*, 53–69. Springer.
- Lai, Y.; Zhou, Y.; Liu, X.; and Zhou, T. 2024. Memory-Assisted Sub-Prototype Mining for Universal Domain Adaptation. In *The Twelfth International Conference on Learning Representations*.
- Li, Z.; and Hoiem, D. 2017. Learning without forgetting. *IEEE transactions on pattern analysis and machine intelligence*, 40(12): 2935–2947.
- Lin, G.; Chu, H.; and Lai, H. 2022. Towards better plasticity-stability trade-off in incremental learning: A simple linear connector. In *Proceedings of the IEEE/CVF Conference on Computer Vision and Pattern Recognition*, 89–98.
- Liu, X.; Wu, C.; Menta, M.; Herranz, L.; Raducanu, B.; Bagdanov, A. D.; Jui, S.; and de Weijer, J. v. 2020. Generative feature replay for class-incremental learning. In *Proceedings of the IEEE/CVF Conference on Computer Vision and Pattern Recognition Workshops*, 226–227.
- Liu, X.; and Zhou, Y. 2024. COCA: Classifier-Oriented Calibration via Textual Prototype for Source-Free Universal Domain Adaptation. In *Proceedings of the Asian Conference on Computer Vision*, 1671–1687.
- Lopez-Paz, D.; and Ranzato, M. 2017. Gradient episodic memory for continual learning. *Advances in neural information processing systems*, 30.
- Luo, S.; Chen, W.; Tian, W.; Liu, R.; Hou, L.; Zhang, X.; Shen, H.; Wu, R.; Geng, S.; Zhou, Y.; et al. 2024. Delving into Multi-modal Multi-task Foundation Models for Road Scene Understanding: From Learning Paradigm Perspectives. *IEEE Transactions on Intelligent Vehicles*.
- Mallya, A.; and Lazebnik, S. 2018. Packnet: Adding multiple tasks to a single network by iterative pruning. In *Proceedings of the IEEE conference on Computer Vision and Pattern Recognition*, 7765–7773.
- McCloskey, M.; and Cohen, N. J. 1989. Catastrophic interference in connectionist networks: The sequential learning problem. In *Psychology of learning and motivation*, volume 24, 109–165. Elsevier.
- Peng, X.; Bai, Q.; Xia, X.; Huang, Z.; Saenko, K.; and Wang, B. 2019. Moment matching for multi-source domain adaptation. In *Proceedings of the IEEE/CVF international conference on computer vision*, 1406–1415.
- Pham, Q.; Liu, C.; and Hoi, S. 2021. Dualnet: Continual learning, fast and slow. *Advances in Neural Information Processing Systems*, 34: 16131–16144.
- Radford, A.; Kim, J. W.; Hallacy, C.; Ramesh, A.; Goh, G.; Agarwal, S.; Sastry, G.; Askell, A.; Mishkin, P.; Clark, J.; et al. 2021. Learning transferable visual models from natural language supervision. In *International conference on machine learning*, 8748–8763. PMLR.
- Razdaibiedina, A.; Mao, Y.; Hou, R.; Khabsa, M.; Lewis, M.; and Almahairi, A. 2023. Progressive prompts: Continual learning for language models. *arXiv preprint arXiv:2301.12314*.
- Rebuffi, S.; Kolesnikov, A.; and Lampert, C. H. 2016. icarl: Incremental classifier and representation learning. CoRR abs/1611.07725 (2016). *arXiv preprint arXiv:1611.07725*.
- Rusu, A. A.; Rabinowitz, N. C.; Desjardins, G.; Soyer, H.; Kirkpatrick, J.; Kavukcuoglu, K.; Pascanu, R.; and Hadsell, R. 2016. Progressive neural networks. *arXiv preprint arXiv:1606.04671*.
- Sheng, L.; Lin, Z.; Shao, J.; and Wang, X. 2018. Avatar-net: Multi-scale zero-shot style transfer by feature decoration. In *Proceedings of the IEEE conference on computer vision and pattern recognition*, 8242–8250.
- Simon, C.; Faraki, M.; Tsai, Y.-H.; Yu, X.; Schuster, S.; Suh, Y.; Harandi, M.; and Chandraker, M. 2022. On generalizing beyond domains in cross-domain continual learning. In *Proceedings of the IEEE/CVF Conference on Computer Vision and Pattern Recognition*, 9265–9274.



- Smith, J. S.; Karlinsky, L.; Gutta, V.; Cascante-Bonilla, P.; Kim, D.; Arbelles, A.; Panda, R.; Feris, R.; and Kira, Z. 2023. Coda-prompt: Continual decomposed attention-based prompting for rehearsal-free continual learning. In *Proceedings of the IEEE/CVF Conference on Computer Vision and Pattern Recognition*, 11909–11919.
- Sun, H.-L.; Zhou, D.-W.; Ye, H.-J.; and Zhan, D.-C. 2023. PILOT: A Pre-Trained Model-Based Continual Learning Toolbox. *arXiv preprint arXiv:2309.07117*.
- Tang, S.; Su, P.; Chen, D.; and Ouyang, W. 2021. Gradient regularized contrastive learning for continual domain adaptation. In *Proceedings of the AAAI Conference on Artificial Intelligence*, volume 35, 2665–2673.
- Tao, X.; Hong, X.; Chang, X.; and Gong, Y. 2020. Bi-Objective Continual Learning: Learning ‘New’ While Consolidating ‘Known’. *Proceedings of the AAAI Conference on Artificial Intelligence*, 34(04): 5989–5996.
- Van de Ven, G. M.; Siegelmann, H. T.; and Tolias, A. S. 2020. Brain-inspired replay for continual learning with artificial neural networks. *Nature communications*, 11(1): 4069.
- Van der Maaten, L.; and Hinton, G. 2008. Visualizing data using t-SNE. *Journal of machine learning research*, 9(11).
- Volpi, R.; Larlus, D.; and Rogez, G. 2021. Continual adaptation of visual representations via domain randomization and meta-learning. In *Proceedings of the IEEE/CVF Conference on Computer Vision and Pattern Recognition*, 4443–4453.
- Wah, C.; Branson, S.; Welinder, P.; Perona, P.; and Belongie, S. 2011. The caltech-ucsd birds-200-2011 dataset.
- Wang, L.; Zhang, X.; Su, H.; and Zhu, J. 2024. A comprehensive survey of continual learning: Theory, method and application. *IEEE Transactions on Pattern Analysis and Machine Intelligence*.
- Wang, Z.; Liu, L.; Duan, Y.; and Tao, D. 2022a. Continual learning through retrieval and imagination. In *Proceedings of the AAAI Conference on Artificial Intelligence*, 8, 8594–8602.
- Wang, Z.; Zhang, Z.; Ebrahimi, S.; Sun, R.; Zhang, H.; Lee, C.-Y.; Ren, X.; Su, G.; Perot, V.; Dy, J.; et al. 2022b. Dual-prompt: Complementary prompting for rehearsal-free continual learning. In *European Conference on Computer Vision*, 631–648. Springer.
- Wang, Z.; Zhang, Z.; Lee, C.-Y.; Zhang, H.; Sun, R.; Ren, X.; Su, G.; Perot, V.; Dy, J.; and Pfister, T. 2022c. Learning to prompt for continual learning. In *Proceedings of the IEEE/CVF Conference on Computer Vision and Pattern Recognition*, 139–149.
- Wu, Y.; Chen, Y.; Wang, L.; Ye, Y.; Liu, Z.; Guo, Y.; and Fu, Y. 2019. Large scale incremental learning. In *Proceedings of the IEEE/CVF conference on computer vision and pattern recognition*, 374–382.
- Xiao, H.; Rasul, K.; and Vollgraf, R. 2017. Fashion-mnist: a novel image dataset for benchmarking machine learning algorithms. *arXiv preprint arXiv:1708.07747*.
- Xie, J.; Yan, S.; and He, X. 2022. General incremental learning with domain-aware categorical representations. In *Proceedings of the IEEE/CVF Conference on Computer Vision and Pattern Recognition*, 14351–14360.
- Yao, L.; and Miller, J. 2015. Tiny imagenet classification with convolutional neural networks. *CS 231N*, 2(5): 8.
- Zhou, D.-W.; Wang, Q.-W.; Ye, H.-J.; and Zhan, D.-C. 2022. A model of 603 exemplars: Towards memory-efficient class-incremental learning. *arXiv preprint arXiv:2205.13218*.

# Appendix

In the supplemental document, we present:

- Evaluation Details
- Details of Empirical Study
- Details of DisCo implementation, evaluation benchmarks, and additional results
- Limitations and Future Work

## A Evaluation Metrics Details

### A.1 Metrics of class incremental learning

Based on the survey (Wang et al. 2024), we evaluate the continual model mainly from two aspects: the overall Average Accuracy  $AA$  and Forgetting Measure  $FM$ .

Let  $a_{k,j} \in [0, 100]$  denote the classification accuracy evaluated on the test dataset of the  $j$ -th task after incremental training of the  $k$ -th task ( $1 \leq j \leq k$ ). The average accuracy at the  $k$ -th task is defined as:

$$AA_k = \frac{1}{k} \sum_{j=1}^k a_{k,j} \quad (8)$$

Furtherly, the overall average performance  $AA$  after all  $T$  tasks is then defined as:

$$AA = \frac{1}{T} \sum_{k=1}^T AA_k \quad (9)$$

For a single task, the forgetting  $f$  is calculated by the difference between its maximum accuracy achieved in the past and its current accuracy after the  $k$ -th task:

$$f_{j,k} = \max_{i \in \{1, \dots, k-1\}} (a_{i,j} - a_{k,j}), \forall j < k. \quad (10)$$

Then  $FM$  after all  $T$  task is the average forgetting of all old tasks:

$$FM = \frac{1}{T-1} \sum_{j=1}^{T-1} f_{j,T-1}. \quad (11)$$

Moreover, to reflect the model performance when learning a new task, we design the Initial Accuracy  $IA$ , which is the average accuracy of each task after its initial training:

$$IA = \frac{1}{T} \sum_{i=1}^T a_{i,i} \quad (12)$$

### A.2 Metrics $PIV$ and $PFTS$

We decouple the model  $f_\theta$  into two parts: the feature extractor  $\mathbf{F}$  parameterized by  $\theta_{\mathcal{F}}$  and the classifier  $\mathbf{W}$  parameterized by  $\theta_{\mathcal{W}}$ . Since we aim to investigate parameters related to features, we represent the parameter update between task  $t$  and task  $t-1$  as  $\Delta\theta_t = \theta_{\mathcal{F}_t} - \theta_{\mathcal{F}_{t-1}}$ . For each task  $t$ , we use  $\mathcal{H}_t = \{i \mid |(\Delta\theta_t)_i| > \delta\}$  ( $\delta$  is the threshold which is set to be the upper quartile value of all parameters' update) to denote the set of indices corresponding to the high-magnitude updates in  $\Delta\theta_t$ . For each pair of tasks  $t$  and  $t'$ , we use  $J(t, t')$

to measure the overlap in parameters they update. Specifically, the interference value  $IS$  is quantified using the Jaccard index (Jaccard 1901), which is a measure of similarity between finite sets:

$$IS = J(t, t') = \frac{|\mathcal{H}_t \cap \mathcal{H}_{t'}|}{|\mathcal{H}_t \cup \mathcal{H}_{t'}|}. \quad (13)$$

When the interference between task  $t$  and  $t'$  is small, the  $IS$  will be correspondingly lower. We then compute the pairwise forward transfer score  $FTS$  as below:

$$FTS(t, t') = J(t, t') \times \left( \frac{\|\Delta\theta_t\|_2 + \|\Delta\theta_{t'}\|_2}{2} \right). \quad (14)$$

This score captures both the overlap and average update magnitude, providing a measurement of knowledge learned by parameters in task  $t$ . The higher  $FTS$  is, the more the model learns at stage  $t$ . Consequently,  $FTS$  can be regarded as the learning plasticity of the model. Then the overall parameter interference value  $PIV$  and overall parameter forward transfer  $PFTS$  is represented as:

$$PIV = \frac{1}{T-1} \sum_{t=2}^T IS(t, t-1) \quad (15)$$

$$PFTS = \frac{1}{T-1} \sum_{t=2}^T FTS(t, t-1) \quad (16)$$

## B Details of Empirical Study

### B.1 Details of the construction of CIL and CILD scenarios

**Synthesizing images of new domains** . We manually add domain shift to the original CIFAR-100 dataset using a style transfer GAN named Avatar-Net (Sheng et al. 2018) to synthesize images of new domains, resulting in a new dataset DomainCIFAR-100. In the official implementation of AvatarNet, the author provides 5 styles: *brush strokes*, *lamuse*, *plum flower*, *woman in peasant dress*, and *candy*. For the original CIFAR-100 which contains 60000 images and 100 labels, we feed it into AvatarNet and get  $5 \times 60000$  images of 5 domains. We split the class space  $[0,99]$  randomly into 6 dis-joint subspaces  $S_i$ , with the first subspace containing 50 classes and the others containing 10 classes respectively. At the same time, we randomly design a 6-domain order  $\mathcal{P}$  such as  $\{\text{real, brush strokes, lamuse, plum flower, woman in peasant dress, candy}\}$ , where *real* means the original style. Then as shown in Fig. 2, we can construct a DomainCIFAR-100 CILD scenario with 6 tasks, each task containing images of one style. The corresponding CIL scenario shares the same subspaces with that of CILD, but all tasks are in the same domain (We choose the first domain in  $\mathcal{P}$  of CILD as the only domain of CIL). By this design, we can simulate the situation where each task is introduced with a new domain while maintaining its image structure to the most extent.

**Splitting DomainNet** DomainNet (Peng et al. 2019) is a popular dataset in transfer learning, spanning over 6 domains: *clipart*, *infograph*, *painting*, *quickdraw*, *real*, and

Method	scenario	CIFAR-100			DomainNet		
		AA $\uparrow$	FM $\downarrow$	backbone	AA $\uparrow$	FM $\downarrow$	backbone
iCaRL	CIL	<b>64.15</b>	46.23	ViT-B/16	52.51	34.19	ViT-B/16
iCaRL	CILD	63.69	<b>22.00(-24.23)</b>	ViT-B/16	<b>56.15</b>	<b>18.05(-16.14)</b>	ViT-B/16
BiC	CIL	68.55	36.60	ViT-B/16	<b>59.22</b>	34.25	ViT-B/16
BiC	CILD	<b>69.03</b>	<b>12.11(-24.49)</b>	ViT-B/16	57.98	<b>16.23(-18.02)</b>	ViT-B/16
MEMO	CIL	75.63	25.44	ResNet-18	76.57	16.35	ResNet-32
MEMO	CILD	<b>76.89</b>	<b>16.10(-9.34)</b>	ResNet-18	<b>78.93</b>	<b>6.87(-9.48)</b>	ResNet-32
LwF	CIL	53.23	43.53	ViT-B/16	<b>48.08</b>	42.16	ViT-B/16
LwF	CILD	<b>54.07</b>	<b>16.26(-27.27)</b>	ViT-B/16	45.00	<b>21.84(-20.32)</b>	ViT-B/16
DER	CIL	64.64	45.15	ResNet-18	72.18	24.63	ResNet-32
DER	CILD	<b>66.37</b>	<b>2.25(-42.90)</b>	ResNet-18	<b>73.49</b>	<b>13.50(-11.13)</b>	ResNet-32

Table 4: Comparative analysis on accuracy(AA) and forgetting(FM) of CIL models under CIL and CILD scenarios after alternating their backbones.

*sketch*, each domain has 345 classes. Similarly, we randomly split the class space [0,344] into 5 dis-joint subspaces  $S_i$ , each subspace has  $345 \div 5 = 69$  classes. We randomly design a 6-domain order  $\mathcal{P}$  such as {real, infograph, painting, quickdraw, clipart, and sketch}. The same as we construct DomainCIFAR-100, we can then construct CILD and CIL scenarios of DomainNet. Compared to DomainCIFAR-100, CILD scenario of DomainNet is more similar to real-world application where both styles and image structures may change significantly in different tasks.

## B.2 Details of empirical study implementation

The backbones of used baselines in section 3.2 are shown in Tab. 5. We train all models from scratch with random

Method	Backbone	
	CIFAR-100	DomainNet
iCaRL	ResNet-18	ResNet-32
BiC	ResNet-18	ResNet-32
MEMO	ViT-B/16	ViT-B/16
LwF	ResNet-18	ResNet-32
DER	ViT-B/16	ViT-B/16
L2P	ViT-B/16	ViT-B/16

Table 5: Backbones of baselines in Empirical Study. We choose these backbones based on the default config of the PILOT repository (Sun et al. 2023).

initialization. The implementation code and training strategy are the same with that of section 5.1.

## B.3 More details of observation

**Observation on different backbones** To validate the generalizability of our observation, we change the backbone and conduct exactly the same experiments as in section 3.2, the result is shown in Tab. 4. We can observe that no matter the backbone type, models under CILD scenario demonstrate better performance than CIL.

**Observation on pre-trained models** For ViT-based models, we use the pre-trained model provided by PILOT (Sun et al. 2023) to initialize our model, and for ResNet-based models, we load the pre-trained resnet weights from pytorch. We conduct the same empirical study as shown in Tab. 6. All models are trained 20 epochs for each task using the backbone type as in Tab. 5. We can get the same observation under this circumstance.

**Observation on first task** As shown in Fig. 6, if we take a close look at just the first task performance during the whole training process, we can observe that models suffer from much less forgetting under CILD.

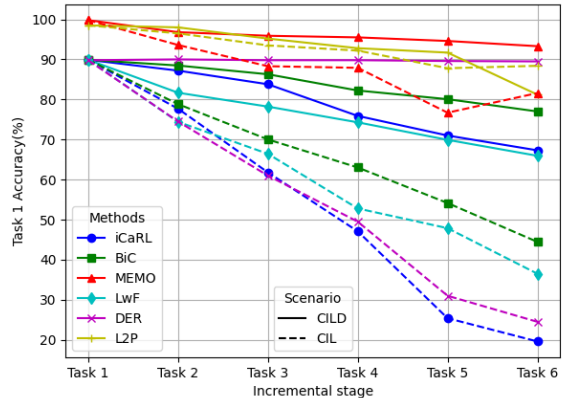


Figure 6: Comparison of accuracy curves of the first task on CIFAR-100. Most continual methods under CILD demonstrate a fantastic low forgetting rate of the first task.

**Observation on different domain orders** The results above in the empirical study are all achieved under the domain order where the first domain is real. We alter the first domain and conduct more experiments. For CIFAR-100, the CILD domain order is:

Method	scenario	CIFAR-100		Backbone	DomainNet		Backbone
		AA $\uparrow$	FM $\downarrow$		AA $\uparrow$	FM $\downarrow$	
iCaRL	CIL	81.51	25.06	ResNet-18	83.62	23.60	ResNet-32
iCaRL	CILD	<b>83.02</b>	<b>8.57(-24.23)</b>	ResNet-18	<b>84.29</b>	<b>9.34(-14.26)</b>	ResNet-32
BiC	CIL	83.24	29.60	ResNet-18	<b>79.26</b>	29.84	ResNet-32
BiC	CILD	<b>85.00</b>	<b>7.67(-21.93)</b>	ResNet-18	76.21	<b>10.25(-19.59)</b>	ResNet-32
MEMO	CIL	<b>90.38</b>	13.29	ViT-B/16	<b>92.06</b>	8.64	ViT-B/16
MEMO	CILD	90.17	<b>7.01(-6.28)</b>	ViT-B/16	88.29	<b>5.49(-3.15)</b>	ViT-B/16
LwF	CIL	<b>74.68</b>	26.89	ResNet-18	<b>70.64</b>	29.16	ResNet-32
LwF	CILD	72.03	<b>14.35(-12.54)</b>	ResNet-18	68.33	<b>16.58(-12.58)</b>	ResNet-32
DER	CIL	<b>87.04</b>	16.29	ViT-B/16	<b>89.18</b>	20.98	ViT-B/16
DER	CILD	86.80	<b>0.40(-42.90)</b>	ViT-B/16	<b>88.22</b>	<b>8.42(-12.56)</b>	ViT-B/16

Table 6: Comparative analysis on accuracy(AA) and forgetting(FM) of pre-trained CIL models under CIL scenario and CILD scenario. ViT-based models load all weights from PILOT (Sun et al. 2023), while ResNet-based models load backbone weight from pytorch.

{brush strokes $\rightarrow$ candy $\rightarrow$ real $\rightarrow$ woman in peasant dress $\rightarrow$ lamuse $\rightarrow$ plum flower},

while the CIL has the only domain brush strokes. For DomainNet, the CILD domain order is:

{quickdraw $\rightarrow$ painting $\rightarrow$ clipart $\rightarrow$ real $\rightarrow$ infograph $\rightarrow$ sketch},

while the CIL has the only domain quickdraw.

We can the same observation in Tab. 7 that these models demonstrate a fantastic lower forgetting rate under the CILD scenario. Moreover, the forgetting rate under CILD scenario in this domain order is comparable or even lower than in the original order. In contrast, most models suffer from worse forgetting under CIL scenario in this domain order.

Method	scenario	CIFAR-100		DomainNet	
		AA $\uparrow$	FM $\downarrow$	AA $\uparrow$	FM $\downarrow$
iCaRL	CIL	52.34	53.67	53.09	55.60
iCaRL	CILD	<b>55.15</b>	<b>23.87(-29.80)</b>	<b>56.21</b>	<b>19.63(-35.97)</b>
BiC	CIL	64.98	43.16	<b>57.30</b>	46.14
BiC	CILD	<b>70.19</b>	<b>15.30(-27.86)</b>	56.77	<b>15.27(-30.87)</b>
MEMO	CIL	<b>84.29</b>	21.44	<b>83.66</b>	16.84
MEMO	CILD	81.67	<b>9.56(-11.88)</b>	79.25	<b>7.98(-8.86)</b>
LwF	CIL	<b>46.28</b>	53.10	<b>44.35</b>	51.20
LwF	CILD	43.76	<b>26.54(-26.56)</b>	42.43	<b>24.22(-26.98)</b>
DER	CIL	58.32	41.26	<b>62.19</b>	34.18
DER	CILD	<b>62.87</b>	<b>1.3(-39.96)</b>	60.36	<b>11.75(-22.43)</b>
L2P	CIL	<b>77.41</b>	<b>11.54</b>	<b>74.21</b>	<b>13.57</b>
L2P	CILD	56.25	23.80(+12.26)	51.07	26.70(+13.13)

Table 7: Comparative analysis on accuracy(AA) and forgetting(FM) of CIL models under CIL and CILD scenarios after alternating the domain order.

**Dive into the “forgetting” of CILD** Forgetting is complex and may not be perfectly reflected by the accuracy drop. In CILD, there is possibility that the model **does not indeed “forget less” its inner knowledge** about classifying

seen categories, but rather **more able to “recall” its memory**. That is to say, there is a chance that adding domain shift may help model identify the task boundary, hence help model “recall” its memory.

Method	Scenario	TIA	ITA – first
iCaRL	CIL	50.14	36.22
	CILD	<b>84.29</b>	<b>79.06</b>
BiC	CIL	51.06	37.64
	CILD	<b>86.22</b>	<b>81.55</b>
MEMO	CIL	84.16	85.12
	CILD	<b>91.06</b>	<b>92.99</b>
LwF	CIL	48.98	42.13
	CILD	<b>85.35</b>	<b>83.83</b>
DER	CIL	82.69	35.12
	CILD	<b>98.67</b>	<b>96.75</b>
L2P	CIL	<b>92.65</b>	<b>90.46</b>
	CILD	81.28	83.69

Table 8: Results of Task-Inference Accuracy(TIA) and (first)Intra-Task Accuracy(ITA) on CIFAR-100. Higher TIA means model is more able to identify task ID, thus being more able to recall its corresponding knowledge. Higher ITA means the model remembers more knowledge about certain classes.

To investigate this, we employ two metrics: Task-Inference Accuracy(TIA) to evaluate the ability to identify task ID(ability to recall memory), and Intra-Task Accuracy(ITA) to evaluate the inner knowledge of model. For TIA, after training of all tasks, we give test sample to the model and see which label space(i.e. inferred task ID) does this predicted class belongs to. For ITA, we isolate the weight of the classifier and treat each of them as the exclusive classifier for each task. We manually feed the sample feature to its corresponding classifier and get its ITA in that

classifier. We only compare the *ITA* of the first task since they share the same test set. From Tab. 8, we can see that domain shift in CILD indeed helps model identify the task boundary. Moreover, *ITA* in CIL is much lower, indicating model does forget what it learned. So, the performance under CILD is not only caused by a clearer task boundary, but also due to forgetting less knowledge.

## C Details of DisCo implementation, evaluation benchmarks, and additional results

### C.1 Datasets Details

- CIFAR100 (Krizhevsky and Hinton 2009) is a classic classification dataset composed of 100 categories, each having 500 training images and 100 test images of resolution  $32 \times 32$  pixels. We follow the setting of previous works (Lopez-Paz and Ranzato 2017; Rebuffi, Kolesnikov, and Lampert 2016) and split the CIFAR100 randomly and evenly into 10 tasks, each task having 10 classes respectively.
- Fashion-MNIST (Xiao, Rasul, and Vollgraf 2017) is a dataset of Zalando’s article images—consisting of a training set of 60,000 examples and a test set of 10,000 examples. Each example is a  $28 \times 28$  grayscale image, associated with a label from 10 classes. The Fashion-MNIST dataset offers a more challenging benchmark than the traditional MNIST due to its more complex and varied patterns, which better mimic real-world data. This increased complexity helps develop and test more robust machine learning models. We split Fashion-MNIST randomly and evenly into 5 tasks, each task containing 2 classes.
- Due to resource limits, we employ Tiny-ImageNet (Yao and Miller 2015) instead of the full ImageNet (Deng et al. 2009) as one of the benchmarks. Tiny-ImageNet is a simplified version of the larger ImageNet, covering 200 classes, and each contains 500 training images, 50 validation images, and 50 test images. The images are downscaled to  $64 \times 64$  pixels, compared to the higher resolutions in the original ImageNet. We split Tiny-ImageNet into 10 tasks randomly and evenly, each task containing 20 classes.

### C.2 Baseline Details

- iCaRL (Rebuffi, Kolesnikov, and Lampert 2016) is a rehearsal-based class incremental learning model, proposing a novel method to choose buffer samples to replay and using KD loss to regulate the logits of old and new models.
- MEMO (Zhou et al. 2022) proposes decoupling the backbone at middle layers into shallow and deep layers and expands deep layers for each task depending on the limited memory buffer.
- BiC (Wu et al. 2019), or **Bias Correction**, is a rehearsal-based model designed to enhance continual learning models by addressing the issue of biased representation

towards newer classes. It does this by introducing a bias correction layer at the end of the learning model, which adjusts the decision boundaries in favor of previously learned tasks.

- LwF (Li and Hoiem 2017) is a regularization-based model that uses knowledge distillation to align the outputs of old and new models without a memory buffer.
- DER (Buzzega et al. 2020) adapt the dynamic structure from Task-Incremental Learning to Class-Incremental Learning, which freezes the old feature model to preserve old knowledge while creating a new trainable feature extractor concatenating their features together to adapt the model to new tasks. Like rehearsal-based methods, DER requires a memory buffer to store old task samples.
- L2P (Wang et al. 2022c) is a recently popular prompt-based method, which leverages the frozen pre-trained vision transformer (Dosovitskiy et al. 2020) with trainable prompts to adapt the model to continual scenarios.

The backbones used by them are the same as those in empirical study, as listed in Tab. 5. For ViT-based methods, we up-sample the original images to  $224 \times 224$  using bicubic interpolation.

### C.3 Incorporating DisCo into prompt-based methods

Prompt-based methods like L2P (Wang et al. 2022c) leverage a frozen pre-trained vision transformer (Dosovitskiy et al. 2020) with a trainable prompt pool to adapt the model to continual scenarios. The prompt pool  $\mathcal{PP}$  is composed of  $M$  key-value pairs  $\mathcal{PP} = \{k_1, v_1\}, \{k_2, v_2\} \dots \{k_M, v_M\}$ , where  $v_i \in \mathbb{R}^{L_p \times d}$  is a prompt with token length  $L_p$  and  $k_i \in \mathbb{R}^d$  is the key attached to it. Given an image input  $x$ , L2P first uses a frozen pre-trained vision transformer  $\phi_0$  to extract the CLS token  $q \in \mathbb{R}^d$ . Then L2Ps use  $q$  as the query to lookup top- $N$  nearest keys  $K = \{k_1, k_2, \dots, k_N\}$  and their corresponding prompts  $V = \{v_1, v_2, \dots, v_N\}$ . The selected prompts  $V \in \mathbb{R}^{(N \times L_p) \times d}$  are appended before the patch embeddings of  $x$  and feed into  $\phi_0$  for classification.

To incorporate DisCo into it, the key idea is the same as that of incorporating DisCo into other methods: find prototype  $P$  of current task  $t$  and push current features towards  $P$  while keeping them away from previous prototypes. However, directly contrasting CLS features of L2P may lead to even worse forgetting as suggested in 3.2. **Instead, we contrast the selected keys  $K$ .**

For a mini-batch of batchsize  $N_b$ , we first count the frequency of each key being selected. We treat the most frequently selected  $N$  keys as “features of current task”. For DisCo-I, we use their average mean as batch-wise prototype  $p_i$ . We impose the same task-level regularization on these keys as in Eq. 3, with  $p_i$  being the positive sample and prototypes of previous tasks as negative samples.

### C.4 Additional results

**t-SNE visualization of incorporating DisCo** We use t-SNE to visualize the features of incorporating DisCo into baseline models, as shown in Fig. 7.



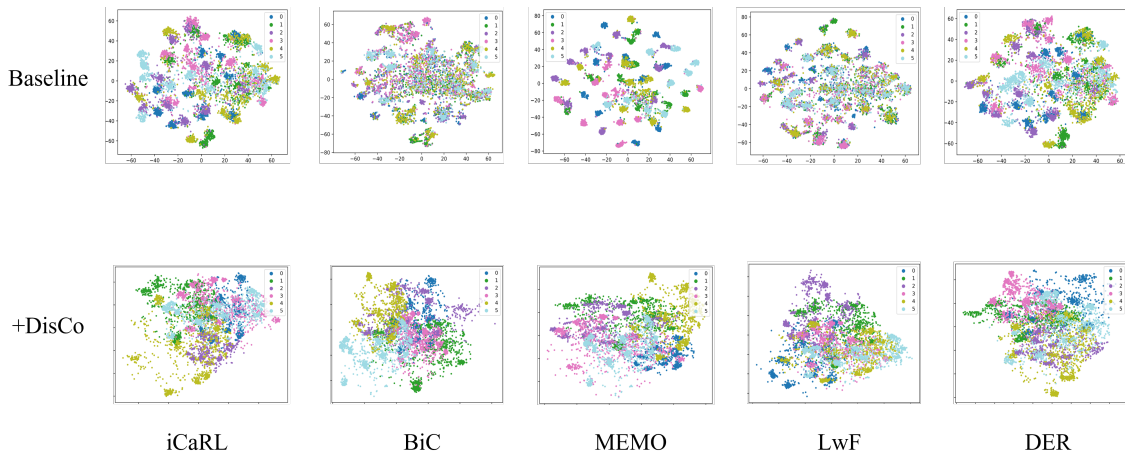


Figure 7: t-SNE visualization of features on CIFAR-100. The top row denotes features extracted by different baseline continual methods and the bottom row denotes features of incorporating DisCo into them. Data points from the same task are marked using the same color.

Method	$AA \uparrow$	$FM \downarrow$
iCaRL	52.06	41.95
iCaRL+DisCo-I	<b>52.43</b>	<b>36.16</b>
BiC	53.98	36.08
BiC+DisCo-I	<b>54.32</b>	<b>33.39</b>
LwF	44.49	46.44
LwF+DisCo-I	<b>46.84</b>	<b>38.99</b>
DER	52.73	36.32
DER+DisCo-I	<b>54.09</b>	<b>34.21</b>
L2P	<b>71.50</b>	<b>8.58</b>
L2P+DisCo-T	71.29	8.97

Table 9: Result of proposed DisCo on fine-grained dataset CUB200(10 classes per task). DisCo succeeds in handling this challenge but its performance boost is restricted due to the blurry task boundary.

We can see that incorporating DisCo yields relatively more distinguishable features, with comparatively more isolated feature distribution for each task.

**Sensitiveness to blurry task boundary** DisCo relies on prototypes, and a blurry task boundary may influence performance. So we evaluate DisCo on CUB200 (Wah et al. 2011), which is a fine-grained classification dataset covering 200 types of birds. As in Tab. 9, DisCo handles this challenge well, reducing forgetting and improving average accuracy. However, it’s worth noting that the  $AA$  improvement and  $FM$  reduction on CUB200 are not that significant compared to the three datasets in the main study Tab. 2. This means blurry task boundaries do have some minor effect on DisCo, which will be a research point for future works.

### C.5 Ablation study on loss weight $\lambda$

In Tab. 10-Tab. 14, we analyze the influence of the weight balance  $\lambda_{tcon}$ ,  $\lambda_{cccon}$  and  $\lambda_{ccd}$  of Eq. 7 on CIFAR-100.

We can see that DisCo achieves a consistently good performance when  $\lambda_{tcon}$  and  $\lambda_{cccon}$  are set to 0.5 and  $\lambda_{ccd} = 1$ . When we amplify  $\lambda_{tcon}$ , which means we impose stricter regularization on task-level distributions, and this will make  $FM$  drop but  $AA$  drops too. This is consistent with the ablation study of different modules in section 5.3.

Method	$\lambda_{tcon}$	$\lambda_{cccon}$	$\lambda_{ccd}$	$AA \uparrow$	$FM \downarrow$
iCaRL DisCo-I	0.5	0.5	1.0	<b>70.11</b>	33.96
	1.0	0.5	1.0	68.56	<b>32.47</b>
	0.5	1.0	1.0	67.44	34.80
	1.0	1.0	1.0	69.16	33.87
	1.0	1.0	0.5	68.64	36.47

Table 10: Evaluation of other possible values of loss weight  $\lambda$  on iCaRL.

Method	$\lambda_{tcon}$	$\lambda_{cccon}$	$\lambda_{ccd}$	$AA \uparrow$	$FM \downarrow$
BiC DisCo-I	0.5	0.5	1.0	<b>69.89</b>	28.54
	1.0	0.5	1.0	67.21	<b>27.34</b>
	0.5	1.0	1.0	66.24	27.67
	1.0	1.0	1.0	62.13	30.16
	1.0	1.0	0.5	61.76	31.01

Table 11: Evaluation of other possible values of loss weight  $\lambda$  on BiC.

Method	$\lambda_{tcon}$	$\lambda_{ccon}$	$\lambda_{ccd}$	AA $\uparrow$	FM $\downarrow$
LwF DisCo-I	0.5	0.5	-	<b>56.42</b>	36.52
	1.0	0.5	-	54.29	<b>34.15</b>
	0.5	1.0	-	55.16	35.98
	1.0	1.0	-	54.60	34.76

Table 12: Evaluation of other possible values of loss weight  $\lambda$  on LwF.

Method	$\lambda_{tcon}$	$\lambda_{ccon}$	$\lambda_{ccd}$	AA $\uparrow$	FM $\downarrow$
DER DisCo-I	0.5	0.5	1.0	<b>64.87</b>	36.41
	1.0	0.5	1.0	60.04	34.83
	0.5	1.0	1.0	64.26	37.11
	1.0	1.0	1.0	62.34	<b>34.57</b>
	1.0	1.0	0.5	59.26	36.98

Table 13: Evaluation of other possible values of loss weight  $\lambda$  on DER.

Method	$\lambda_{tcon}$	$\lambda_{ccon}$	$\lambda_{ccd}$	AA $\uparrow$	FM $\downarrow$
L2P DisCo-T	0.5	0.5	-	83.12	6.80
	1.0	0.5	-	82.39	<b>6.65</b>
	0.5	1.0	-	83.01	6.83
	1.0	1.0	-	<b>83.65</b>	6.76

Table 14: Evaluation of other possible values of loss weight  $\lambda$  on L2P.

## D Limitations and Future Work

Our work draws inspiration from the counter-intuitive phenomenon that CIL models demonstrate lower forgetting rate when introducing domain shifts to each task. We use contrastive learning to implicitly simulate this process at the feature level instead of the input level, and this may be not exactly identical to the phenomenon we discover. In the future, we may explore how to use domain shifts explicitly at the input level. For example, we can incorporate some generative networks in our model to insert domain shift into each task. Moreover, at inference time, we need to find a good way to decide which task this sample belongs to, so that it will be easier to decide which domain shift(or which condition) to give to the generative networks.